Estimation of the reaction kinetic parameters of a mimosa tannin-based thermoset resin with a simulation approach

V. Nicolas, Z. Marie, A. Mija, A. Celzard, V. Fierro

Estimation of the reaction kinetic parameters of a mimosa tannin-based thermoset resin with a simulation approach

V. Nicolas[a], Z. Marie[a], A. Mija[b], A. Celzard[a], V. Fierro[a]

[a] Université de Lorraine, CNRS, IJL, F-88000 Epinal, France

[b] University Côte d'Azur, Institute of Chemistry of Nice, UMR CNRS 7272, 06108 Nice Cedex 02, France

Corresponding Author: vincent.nicolas@univ-lorraine.fr

Abstract

This study presents the estimation of the parameters of the polymerization kinetics of a mimosa tannin-based thermosetting resin. A dual approach, experimental and numerical, was used. The numerical approach consisted in solving a time-dependent 0D numerical model of the polymerization kinetics and the heat equation. Thus, the parameters were estimated by minimizing the difference between the measured and the simulation values for four different polymerization kinetics. During the mixing phase, the temperature was recorded in order to observe the impact of the mixer and the introduction of the polymerization catalyst on the temperature. The modeling showed that the reaction starts directly with the introduction of the catalyst and that this data should not be neglected in order to achieve the minimization. A numerical study on the effect of the simulation time showed a very limited impact on the estimation of the parameters. A simulation time of 350 s was chosen in order to better take into account heat losses. The four polymerization kinetics were consistent with the experimental data and the fit improved from kinetics #1 to kinetics #4 as the number of fitting parameters increased, but the results were of the same order of magnitude. In conclusion, this work presents a simple method from an experimental point of view but very effective for estimating the reaction kinetic parameters of a thermosetting resin based on mimosa tannin. The method can probably be adapted to other polymer systems.

Keywords: Bio-based materials; simulation; reaction kinetics parameters; estimation parameters; tannin

Highlights

- The polymerization kinetics of a mimosa tannin-based resin were determined
- A dual approach, experimental and numerical, was used to find the kinetics parameters
- The simulation must start as soon as the catalyst is introduced
- All four polymerization kinetics provided results consistent with the experimental data
- The polymerization kinetics having 8 parameters best fits the experimental data

1. INTRODUCTION

Rigid polymeric foams are used in a variety of applications, from the automotive field to buildings or appliance insulation. Until recently, these foams were mainly based on phenolic or polyurethane resins, or on polyolefin or PVC thermoplastics. However, foams of biological origin, derived from tannins, could offer an interesting and realistic alternative to petrochemical foams. Tannins are phenolic constituents that can be found in different parts of plants such as leaves, fruits, shells and in particular in the wood and bark of trees (Sjöström, 1993). Condensed tannins are the most studied tannins and can be extracted from different trees such as mimosa (*Acacia mearnsii*), spruce (*Picea abies*), pine (*Pinus radiata* and *Pinus pinaster*), quebracho (*Schinopsis balansae* and *Schinopsi lorentzii*), and larch (*Larix gmelinii*) (Basso et al., 2013; Čop et al., 2014; Lacoste et al., 2015, 2014; Li et al., 2019; Zhou et al., 2019). These tannins are mainly extracted from crushed bark and heartwood using a solvent, generally hot water with a little sodium bisulfate added, in an autoclave. The resultant liquid is then filtered and evaporated by spray drying to finally obtain a fine brown powder. The low manufacturing costs, availability and non-toxicity of these natural resources have increased the use of tannins to develop new materials that can compete with synthetic foams of petrochemical origin.

The exothermic nature of the polymerization reaction between tannin, formaldehyde, furfuryl alcohol and *para*-toluenesulfonic acid (pTSA) produces a foam by boiling and vaporization of a blowing agent (Marie et al., 2019), such as diethyl ether (DEE) (Figure 1).

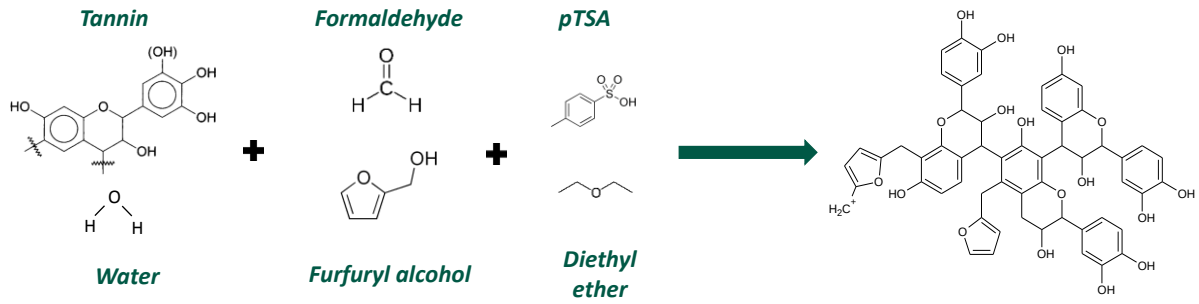

Figure 1: Reaction scheme of thermoset foams based on mimosa tannin. The polymerized structure shown is only one representative example among a large number of other possibilities.

Such a way of preparation is known as physical foaming. The generation of gas inside the tannin-based thermoset resin thus produces its expansion. In parallel, as the polymerization progresses, the viscosity of the reaction medium increases sharply until the resin hardens and sets the final porosity. The reader can easily imagine that this process is similar to baking a cake where the baking time must be carefully chosen to avoid its collapse during cooling (Tondi et al., 2009). Back to the laboratory bench, it can be concluded that the characterization and perfect control of the polymerization phenomenon is essential to control the production of tannin-derived foams. Indeed, if the polymerization starts too early, the porosity cannot be developed; if the polymerization is too late, the porous structure cannot be stabilized and collapses before becoming rigid (Basso et al., 2013a; Basso et al., 2013b; Basso et al., 2013c; Basso et al., 2015).

The foaming of tannin-based thermoset resins has been modelled by a numerical approach in order to optimize their formulations and manufacturing process (Marie et al., 2020). However, to allow the modelling of phenolic resins foaming, the latter study showed a lack of input data concerning the evolution of viscosity and the extent of polymerization. A first-order kinetics was proposed for the polymerization reaction and was introduced into a general foaming model. Thus, the trends in temperature changes and foam deformation were adequately predicted, but there was an overestimation of the final expansion and an underestimation of the heat generated by the exothermic reactions that govern the foaming mechanisms. These differences between the modelling and the experiment highlighted the need to better define the polymerization kinetics and the resulting heat release. As we were

convinced that it was possible to do better, the aim of this new work was to improve our predictions by determining the reaction kinetics.

The determination of the polymerization kinetics as well as the value of the enthalpy of reaction is often carried out by differential scanning calorimetry (DSC) (Guigo et al., 2007). However, DSC is not suitable for tannin-derived thermoset resins due to their rapid polymerization reaction. When the reacting mixture is prepared, exothermic reactions start suddenly and some heat is released before the mixture is poured into the crucible of the instrument, and hence before data acquisition begins. To overcome these difficulties, at least partially, a measurement protocol was established here to monitor temperature changes and determine the polymerization kinetics by fitting the temperature evolution with a numerical model. The final objective was to find the parameters of the polymerization kinetics in order to minimize the difference between predicted and experimental laws.

This protocol included the measurement of the temperature in the bulk of the thermoset resin in the absence of blowing agent. We therefore assumed that the blowing agent is a chemically inert component, which does not participate in polymerization reactions. This is actually the case as we here deal with a physical foaming. In parallel, a 0D numerical model was developed to simulate the temperature and the progress of the reaction using the four laws of polymerization presented in the next section.

2. MATERIALS AND METHODS

2.1. Formulation and temperature acquisition

The device used to follow the evolution of the temperature of the tannin-based thermoset resin over time is now described. A "standard"-type, tannin-based, resin containing all the reagents with the exception of the blowing agent (Basso et al., 2013a; Marie et al., 2020) was used here, and its composition is presented in Table 1.

First, the tannin was dissolved in water with furfuryl alcohol and formaldehyde by mechanical stirring. The stirring speed was set at about 400 rpm for 150 s in a first beaker. The pTSA was then added and incorporated for 30 s under vigorous stirring at more than 1000 rpm before being rapidly poured into the reaction cell of the experimental device. Thus, the reaction process was carried out in two stages, a "mixing" stage (in a beaker of height 4 cm and diameter 3 cm) and a "reaction and cooling" stage (in a beaker of height 10 cm and diameter 6 cm), in order to get as close as possible to the protocol used in the manufacture of the foam.

Table 1 : “Standard” formulation used for the polymerization tests

Constituents	Mass (g)
Mimosa extract tannin (base of the resin)	12
Water (solvent)	2.4
Furfuryl alcohol (co-monomer and heat generator upon polymerization)	4.2
Formaldehyde (37% in water, crosslinker)	2.96
para-toluenesulfonic acid (pTSA, 65% in water, catalyst)	4.4

During these two steps, temperature recording was made when the reaction started well before pouring the formulation into the reaction beaker. Indeed, it is very likely that the reaction begins with the incorporation of pTSA into the reaction mixture, which is followed by 30 seconds of stirring. Taking into account the time required to pour the formulation into the mold and the time to introduce the thermocouple in the solution, a recording time of between 30 and 50s is missing. During this time, data recording is not possible although the first moments of polymerization are crucial and rich in information to determine the

polymerization kinetics of the system. This is an important issue to overcome. For this reason, during the “mixing stage”, a thermocouple type T was placed along the inner wall of the beaker to record temperatures without being affected by stirring. Then, during the "reaction and cooling" phase, another thermocouple type T was immersed in the resin to record the temperature during polymerization and cooling (Figure 2).

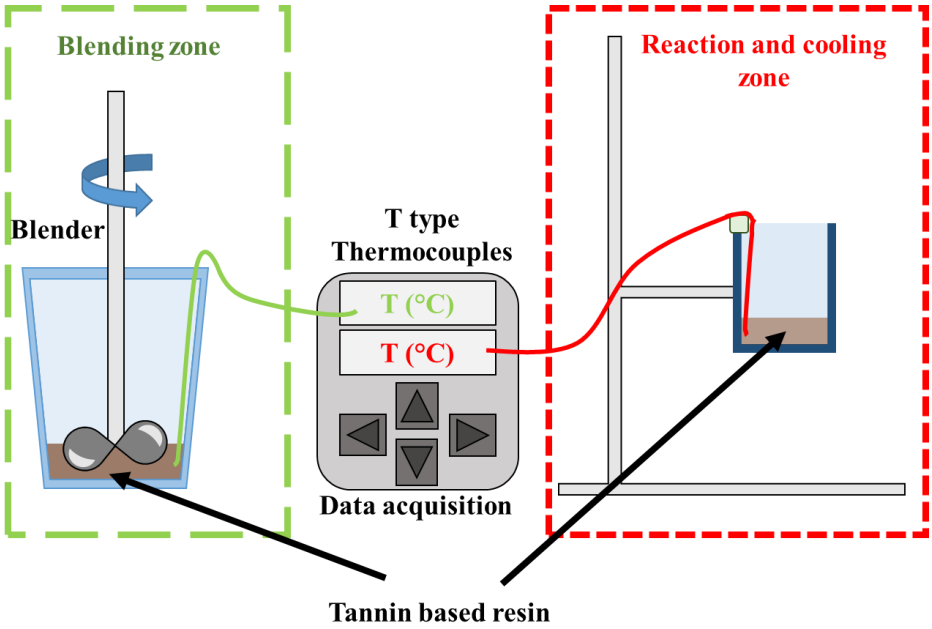

Figure 2: Schematic representation of the continuous temperature measurement protocol during the mixing and polymerization phase

2.2. Reaction modeling

This section focuses on the numerical model developed to determine the polymerization kinetics of our reaction system. Indeed, the polymerization of tannin for foaming involves a multitude of reactions, which are more or less favored by thermal conditions. The reaction of tannins with formaldehyde is often the only reaction taken into account in the crosslinking of tannin-based thermoset resins. However, the exothermic self-condensation reaction of furfuryl alcohol in the presence of acid, which results in the production of furanic polymer chains, is also important, together with the reaction of furfuryl alcohol with tannin oligomers. The reaction mechanisms are therefore more complex and the approach proposed here aims to

define a general law encompassing all the phenomena in order to feed a numerical model. Our reaction modelled was the so-called "standard" formulation (Table 1) but without blowing agent (diethyl ether), which is inert.

For this, a 0D numerical model was developed with Comsol Multiphysics in order to simulate the temperature and the progress of the polymerization reaction within the initially liquid formulation. We aimed to determine, by minimizing the deviation from the experimental temperature, the coefficients of a polymerization law and the associated enthalpy of reaction. As the test mold was thin and the heat generated was large relative to the volume of phenolic resin considered, it was assumed that during exothermic reactions, the temperature was homogeneous inside the mold.

2.2.1. *Equation of extent of reaction*

During foaming, the matrix surrounding the gas bubbles polymerizes as it expands. This polymer matrix is initially liquid and its viscosity gradually increases with the reaction and finally becomes rigid.

Several approaches have been proposed to model the reaction phenomenon for different foams (epoxy, polyurethane etc.). During the reaction of polyurethane foams, an approach based on the conversion of polyol, X_p, and governed by an Arrhenius law, has been proposed (Baser and Khakhar, 1994a, 1994b; Ferkl et al., 2016; Geier et al., 2009; Karimi et al., 2017, 2016; Seo and Youn, 2005). It reads:

$$\frac{\partial X_p}{\partial t} = A_p \exp\left(-\frac{E_p}{RT}\right)\left(1-X_p\right)\left(c_{c,0} - 2c_{w,0}X_w - c_{p,0}X_p\right) \quad (1)$$

where A_p (s^{-1}) is the pre-exponential factor, E_p ($J.mol^{-1}$) is the activation energy, R is the universal gas constant (8.314 $J.mol^{-1}.K^{-1}$) and T (K) is the temperature. $c_{c,0}$, $c_{p,0}$ and $c_{w,0}$ ($mol.m^{-3}$) are the initial concentrations of isocyanate groups, polyol groups and water,

respectively. Finally, X_w is the conversion of water molecules, which react with isocyanate to form a urea bond and carbon dioxide.

Most complete model approaches include a system of partial differential equations describing the reactions taking place in the polymer to calculate the gelation rate (Al-Moameri et al., 2015; Ghoreishi et al., 2014; Shen et al., 2014; Zhao et al., 2014, 2013; Zhao and Suppes, 2015). However, a perfect knowledge of the existing reactions is required, such as:

$$\frac{dc_{iso}}{dt} = -r_{gel} - r_{blow} \quad (2)$$

$$\frac{dc_{OH;i}}{dt} = -r_{gel;i} \quad (3)$$

$$\frac{dc_{water}}{dt} = -r_{blow} \quad (4)$$

$$\frac{dc_{ure}}{dt} = r_{gel} \quad (5)$$

$$\frac{dc_{CO_2}}{dt} = r_{blow} \quad (6)$$

where c_{iso} is the concentration of isocyanate, $c_{OH;i}$ the concentration of hydroxyl groups of polyol i, c_{water} the concentration of water, c_{ure} the concentration of urethane, c_{CO2} the concentration of carbon dioxide, $r_{gel;i}$ the gel reaction rate of polyol i, r_{gel} the summation of gel reaction rates of polyol mixtures, and r_{blow} the blowing reaction rate.

In the present study, which is only a first approach, this type of methodology cannot be used since not all reactions are known in our system.

Other authors chose a more global approach to calculate the extent of polymerization reaction, ξ (dimensionless).

193 Table ***2*** shows the different polymerization kinetics used to simulate the polymerization
194 reactions, depending on the authors and the types of foam used (polyurethane or epoxy).
195
196 **Table 2 :** Kinetic equations used to account for the extent of the polymerization reaction

Name	Equation	Type of foam and reference
Kinetics #1	$\frac{\partial \xi}{\partial t} = A_0 \xi^m \left(1-\xi\right)^n$	*Polyurethane* (Abdessalam et al., 2015; Bikard et al., 2007, 2005; Dimier et al., 2002; Piloyan et al., 1966).
Kinetics #2	$\frac{\partial \xi}{\partial t} = A_0 \exp\left(-\frac{E_0}{RT}\right) \xi^m \left(1-\xi\right)^n$	*Epoxy* (Bourdon et al., 2008; Rao et al., 2012); *Polyurethane* (Gupta and Khakhar, 1999; Marciano et al., 1986, 1982; Piloyan et al., 1966)
Kinetics #3	$\frac{\partial \xi}{\partial t} = \left(A_0 \exp\left(-\frac{E_0}{RT}\right)\right)\left(A_1 + \xi^m\right)\left(1-\xi\right)^n$	*Polyurethane* (Rao et al., 2018, 2017)
Kinetics #4	$\frac{\partial \xi}{\partial t} = \left(k_1 + k_2 \xi^m\right)\left(1-\xi\right)^n$	*Polyurethane* (Ireka et al., 2015)

197
198 These kinetic laws can be expressed by a more general equation introducing 8 parameters
199 (A_0, A_1, A_2, E_0, E_1, E_2, m and n) as follows:

200 $$\frac{\partial \xi}{\partial t} = k_0 \left(k_1 + k_2 \xi^m\right)\left(1-\xi\right)^n \quad (7)$$

with, for i = 0 to 2, $k_i = A_i \exp\left(\frac{-E_i}{RT}\right)$, where A_i, E_i, R and T have the same meaning as in Eq. (1), and where m and n are constants varying from 0 to 3.

The studies cited in Table 2 highlighted that the polymerization laws depend on the progress of the polymerization and on the temperature. In order to determine a specific law corresponding to our reaction system, different equations have been tested as a function either of the progress of the polymerization alone, or of the couple temperature - progress of the polymerization. The general polymerization equation is written as follows:

$$\frac{d\xi}{dt} = f\left(\xi, T\right) \tag{8}$$

2.2.2. *Equation of heat transfer*

The temperature was obtained by developing a simplified physical model taking into account the polymerization reaction of the thermoset resin. For this, we have defined a 0D numerical model that depends on the progress of polymerization ξ, temperature T (assumed homogeneous within the mold), and time t.

The temperature variation during polymerization is due to the generation of heat by exothermic reactions and to the heat exchange with the outside environment. Thus, for each of the polymerization laws tested, the temperature variation was defined by the following equation:

$$\frac{dT}{dt} = -\frac{\Delta H_{pol}}{C_p}\frac{d\xi}{dt} + h_T\frac{\left(T_a - T\right)}{m_r C_p} \tag{9}$$

where h_T (W.K^{-1}) is the equivalent heat exchange coefficient, T_a (K) is the ambient air temperature, m_r (kg) is the mass of thermoset resin, ΔH_{pol} (J.kg^{-1}) is the enthalpy of the polymerization reaction, and C_p (J.kg^{-1}.K^{-1}) is the heat capacity of the thermoset resin.

2.2.3. *Least squares optimization*

The coefficients and enthalpy of polymerization of the chemical reaction were optimized by the Comsol Multiphysics parameter estimation module, the convergence criterion being the minimum difference between the simulated temperature and the experimental temperature using the least squares method. Thus, the chosen polymerization law will be the one whose objective function, *Obj*, is minimal. As indicated by Eq. (10), *Obj* is the quadratic sum of the differences between simulated (T_{sim}) and experimental (T_{exp}) temperatures:

$$Obj = \sum_{i=1}^{N} (T_{sim}(t_i) - T_{\exp}(t_i))^2 \quad (10)$$

where N is the number of experimental points and t is the time.

The coefficients of the polymerization law were defined as parameters to be fitted by applying a SNOPT-type algorithm that allows a function with several variables to be minimized. SNOPT uses a sequential quadratic programming (SQP) algorithm that obtains search directions from a sequence of quadratic programming sub-problems (Gill et al., 2002). Each QP sub-problem minimizes a quadratic numerical model of a certain Lagrangian function subject to a linearization of the constraints.

3. RESULTS AND DISCUSSION

3.1. Experimental temperature evolution

Figure 3 shows the evolution of temperatures in the thermoset resin during mixing and reaction, recorded as described above. Firstly, a slight temperature increase of about 2 °C was

recorded during the homogenization of the reagents (mixing phase), before the introduction of pTSA. Since it is assumed that no reaction takes place without pTSA, this heating should come from the energy supplied by the mechanical stirrer. This small temperature variation is difficult to avoid with the current experimental system, which we wanted to keep as simple and as functional as possible.

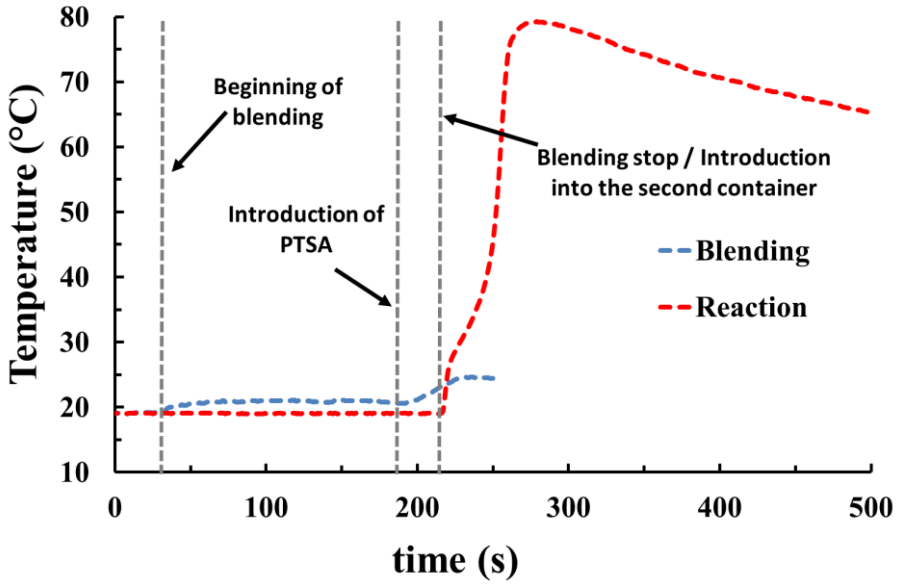

Figure 3: Evolution of the temperature as a function of time within the mixing container (blue) and the reaction container (red).

Figure 3 also shows that the release of heat, due to exothermic reactions, begins a few seconds after the addition of pTSA. The temperature increases exponentially as the formulation is mixed until the resin is poured into the reaction container, where the curing reaction continues. Recording the change in temperature over time in the mixing container has provided a better understanding of what happened at the very beginning of the polymerization. Thus, Figure 4 shows the addition of these two temperature curves (blending and reaction), which has led to a better understanding of the polymerization kinetics.

The conclusions previously put forward for the evolution of foam temperatures can be found. One can note a frank and rapid increase in temperature due to the release of heat by

exothermic reactions up to 80 °C at 90 s and a slow decrease, which seems to tend towards room temperature when the polymer formed cools down. The latter point cannot be confirmed since the experiments were stopped a few minutes after the end of the heat release because we focused on the polymerization phenomenon. In Figure 4, a temperature of 65 °C was recorded 260 s after the maximum temperature.

This study also shows that, when the reaction mixture was poured, the polymerization reactions were largely initiated, which necessitates the assumption of an initial temperature above room temperature and a certain degree of polymerization progress, which is difficult to measure. This is even truer as the polymerization reactions are rapid, especially when they are catalyzed reactions, as it is the case here in the presence of pTSA.

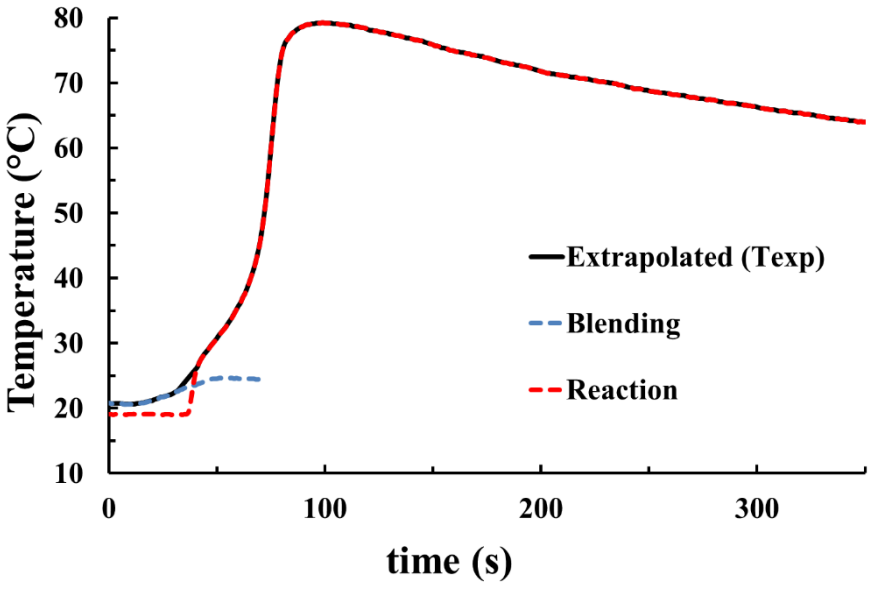

Figure 4 : Definition of the extrapolated temperature (black line), obtained by adding the temperature inside the mixing container (blue dashed line) and the temperature inside the reaction container (red dashed line).

3.2. Determination of the parameters of the extent of reaction equations

In order to determine the kinetics parameters, specific to our reactions mechanism, different polymerization kinetics were tested in a simple model that only calculated the

evolution of temperature and the extent of the thermoset resin reaction over time. The objective was to compare the experimental and the predicted temperature in order to select the best kinetics and then the corresponding kinetics parameters.

Table 3 shows the fixed parameters such as resin mass, specific heat capacity, atmosphere temperature, initial temperature at the introduction of the pTSA and initial extent of the reaction, which was set to zero.

Table 3 : Fixed properties and initial conditions

Properties and inital condition	**Value or expression**
C_p, heat capacity ($J.kg^{-1}.K^{-1}$)	$2500 - 820\ \xi$ *
m_r, mass of the thermoset resin (g)	10.2
T_a, ambient temperature (°C)	19.8
T_0, initial temperature (°C)	20.8
ξ_0, initial extent of reaction (°C)	0

* estimated from a mixing rule based on DSC measurements carried out on more or less polymerized thermoset resins

3.2.1. *Study of impact of the experimental time*

First of all, a study was carried out to observe the impact of the experimental time considered for the simulation on the parameters set for Kinetics #2, which is the most widely used in the open literature and depends only on temperature and the progress of the reaction. Since the temperature reaches a maximum at 100 s but we recorded the temperature up to 350 s, we used several values of experimental times between 100 s and 350 s (i.e., 100, 125, 150, 200, 250, 300 and 350 s). The impact of the latter on the parameters of the polymerization law is shown in Figure 5.

294 This study shows a small impact of the experimental time considered on the majority of
295 the parameters (Figure 5). Indeed, for Kinetics #2, 4 parameters out of 6 have a relative
296 standard deviation of less than 2.4%. The parameters with the greatest variability are the
297 coefficients n and h_T, respectively 9.1 and 9.70%. Moreover, by observing the evolution of
298 these parameters with the experimental time, no obvious trend is observed except for h_T and n,
299 which slightly decreased and increased, respectively, by increasing the duration taken into
300 account. For h_T, this tendency might indicate that heat losses are better taken into account in
301 our study. Concerning, ΔH_{pol} (Figure 5e), we can observe that it is approximately constant
302 after 150 s. Therefore, the other kinetics were applied to the entire recording time (350 s).
303

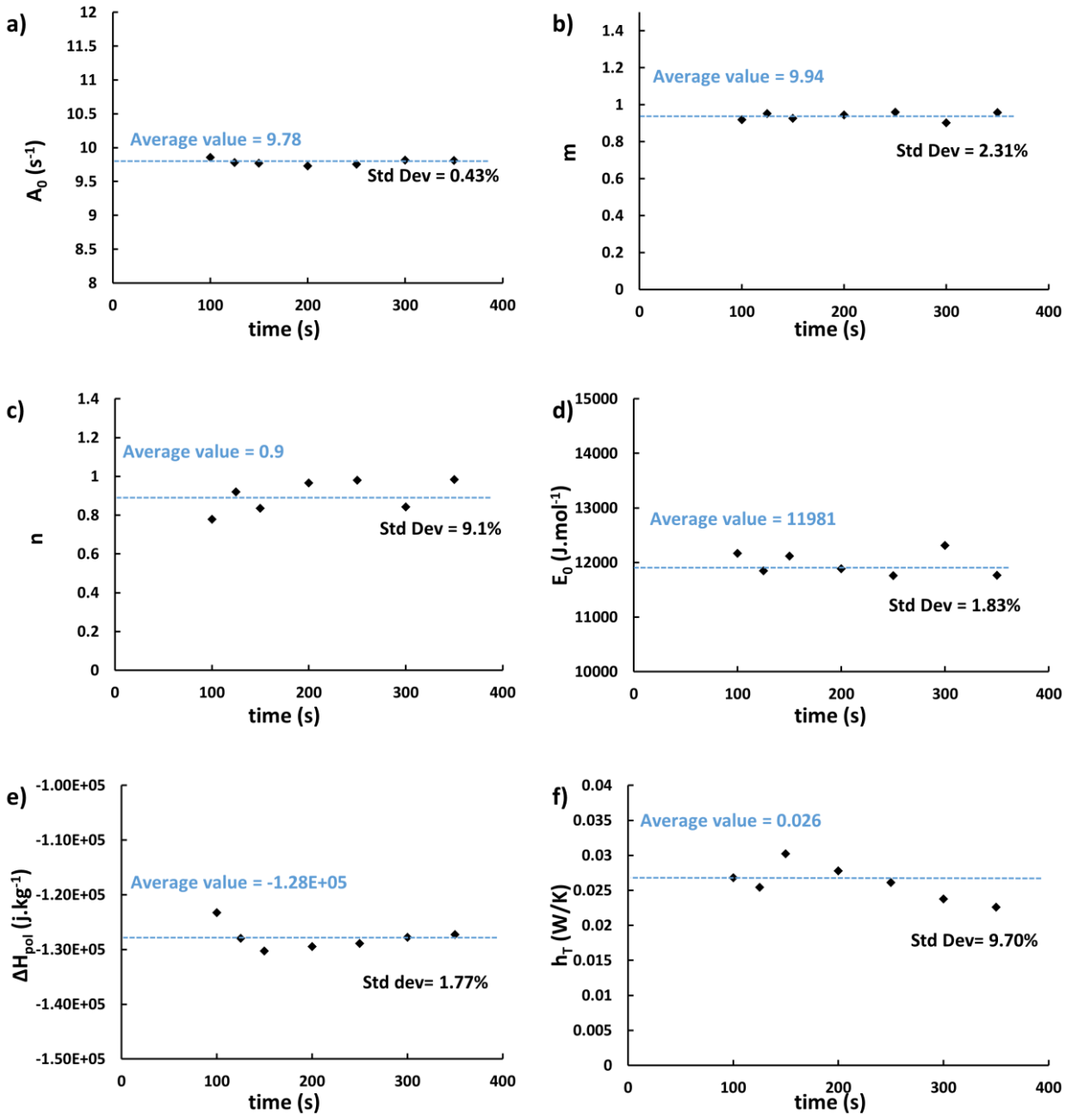

Figure 5 : Evolution of the parameters of Kinetics #2 as a function of the simulation time for the following parameters: (a) A_0; (b) m; (c) n; (d) E_0; (e) ΔH_{pol}; and (f) h_T.

3.2.2. *Results for reaction kinetics.*

Table ***4*** shows m, n, H_{pol} and h_T for the four kinetics considered, and Figure 6 shows the experimental and predicted temperatures. It is evident that the fit improves from Kinetics #1

to Kinetics #4 as the number of fitting parameters increases, but the results are of the same order of magnitude with a relative standard deviation equal to 13.0% for *m*, 5.4% for *n*, 1.3% for H_{pol} and 6.3% for h_T. The reaction order, *m*, is equal to 1, which is higher than values found in the literature for polyurethane: 0.2 (Rao et al., 2018), 0.3 (Bikard et al., 2005), 0.5 (Ireka et al., 2015), 0.8 (Abdessalam et al., 2015; Dimier et al., 2002), and for epoxy: 0 (Rao et al., 2012). The reaction order, *n*, is about 0.9 – 1 in our study, which is somewhat lower than what was found for polyurethane, between 1.2 and 2 (Abdessalam et al., 2015; Bikard et al., 2005; Dimier et al., 2002; Ireka et al., 2015; Rao et al., 2018), or epoxy: 1.4 (Rao et al., 2012). The h_T values seem consistent since it corresponds to a convective exchange coefficient equal to 2.8 $W.m^{-2}.K^{-1}$, which is the order of magnitude for natural convection.

Table 4 : Estimated parameters for the four kinetics tested

Name	A_0 (s^{-1})	A_1 (s^{-1})	A_2 (s^{-1})	E_0 ($J.mol^{-1}$)	E_1 ($J.mol^{-1}$)	E_2 ($J.mol^{-1}$)	*m*	*n*	H_{pol} ($J.kg^{-1}$)	h_T ($W.K^{-1}$)	*Obj*
Kinetics #1	0.129	0	1	0	0	0	1.07	0.885	-1.26E+05	2.13E-2	408.35
Kinetics #2	9.811	0	1	11765	0	0	0.957	0.984	-1.27E+05	2.26E-2	299.81
Kinetics #3	11.185	0.001	1	11707	0	0	1.04	0.943	-1.25E+05	2.05E-2	277.92
Kinetics #4	1	6.961	9.978	0	22813	10879	1.29	1.001	-1.24E+05	1.95E-2	225.22

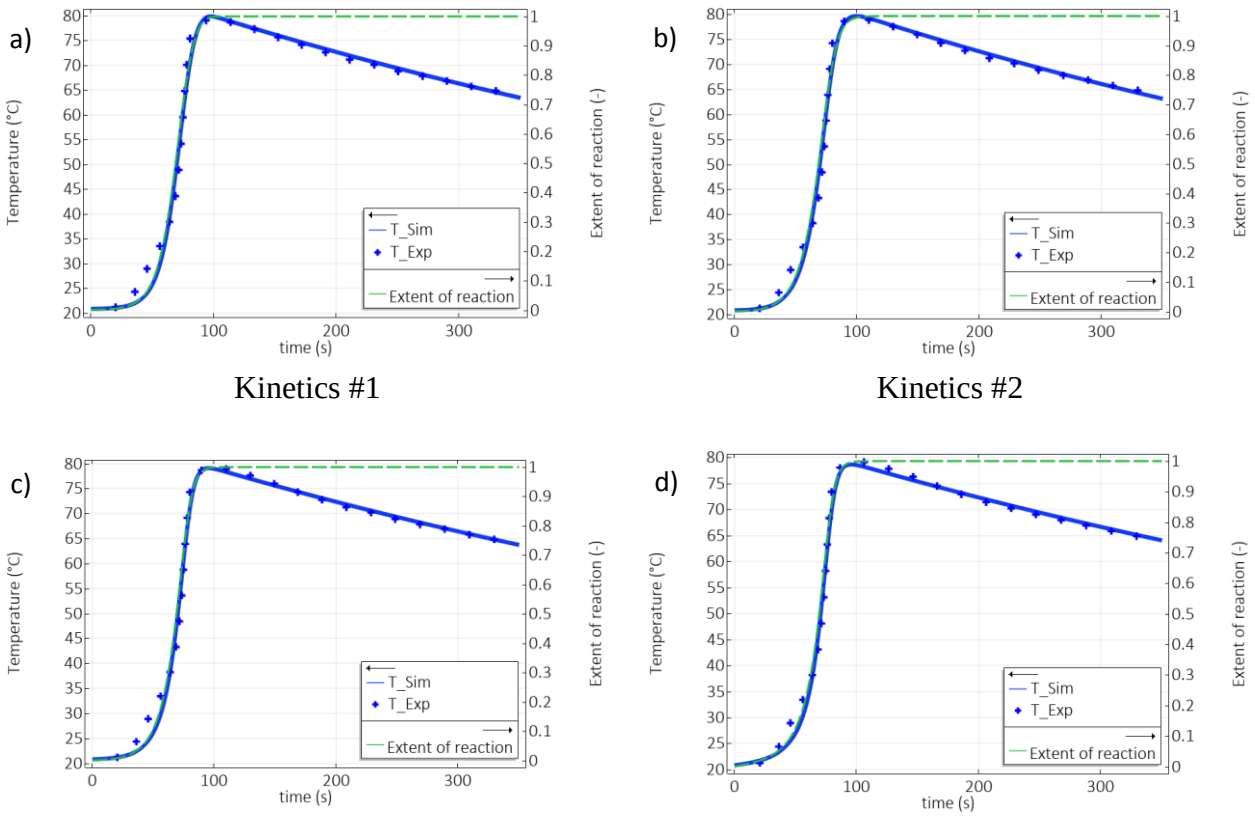

Figure 6 : Evolutions of simulated temperature (blue solid line) and extent of reaction (green dashed line), and of experimental temperature (blue plus sign) for: (a) Kinetics #1 (a); (b) Kinetics #2; (c) Kinetics #3; and (d) Kinetics #4.

Figure 6 also shows that the four polymerization kinetics were able to predict temperature changes over time. Thus, the maximum temperature corresponds to complete polymerization (when the extent of reaction, ξ, reaches the value of 1), the heat released is therefore zero and the foam starts to cool from this moment.

Figure 7 shows the evolution of the objective function at each measurement and for each kinetics. In order to obtain a more in-depth overview of the different numerical models, the sum of the objective functions over the experimental time is also shown in .

Table *4*.

The evolution of *Obj* over time shows that the kinetics deviated the most from the experiment for times between 40 and 90 seconds, which corresponds to the stepwise increase in temperature due to the polymerization reaction. It can be observed that Kinetics #4 shows less variation than the other kinetics, which tends to confirm the better estimate of the parameters with Kinetics #4.

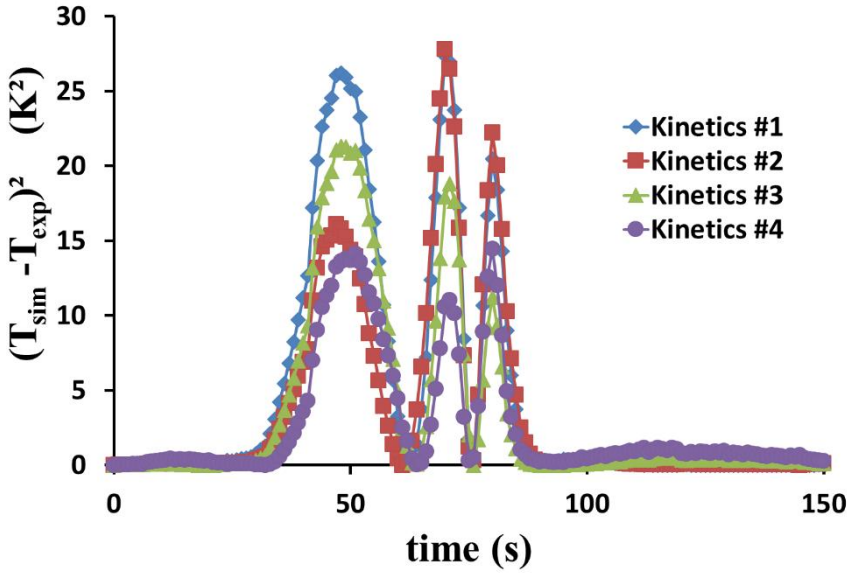

Figure 7 : Objective function for each measurement point for Kinetics #1 (blue line with diamonds), Kinetics #2 (red line with squares), Kinetics #3 (green line with triangles) and Kinetics #4 (purple line with circles). Data are presented up to times of 150 s only for clarity purposes, as there is no significant variation for longer times.

The four kinetics proposed for the polymerization law might be used in a future modeling work, such as the simulation of the foaming kinetics of thermosetting tannin foams. Obviously, if the objective is to maintain maximum accuracy, Kinetics #4 should be used as a priority. However, in some cases where numerical problems may arise, a kinetics with fewer parameters, such as Kinetics #2 and #3, would be of interest in order to simplify the simulations. Finally, in case the simulation should be decoupled from the temperature, Kinetics #1 might be used.

4. CONCLUSION

Simulation of resin thermosetting and foaming of tannin-based formulations is a relevant challenge to pave the way for the paradigm shift in the chemical industry from petrochemicals to biomass feedstocks. In order to find the parameters of the polymerization reaction of tannin-based thermoset resins, a dual experimental and numerical approach was developed. By minimizing the differences between the numerical model and the experimental evolution, the parameters of several polymerization laws were found.

As expected, the experimental study showed that the reaction starts when pTSA is added, which means that the numerical model, by which the kinetics parameters can be found, must start the simulation at this moment and not at the time of pouring. A preliminary study on the impact of the experimental time taken into account showed that the majority of the parameters were practically unaffected. In order to use all the available data, the parameters have been estimated with the longest calculation time (350 s).

Four kinetics describing the progression of the polymerization reaction were then tested, Kinetics #1 being the law with the fewest parameters (5 parameters), and Kinetics #4 being the model with the most parameters to be estimated (8 parameters). Kinetics #4 showed the best results with a sum of the objective function divided by about half, compared to Kinetics #1. It can be highlighted that the four models offer similar results, with a fitting close to the experimental evolution. The kinetics parameters obtained in this study will be introduced into a general model to simulate the expansion of tannin-based foams in a future study.

Acknowledgement

This study was partly supported by TALiSMAN project, funded by FEDER (2019-000214).

5. REFERENCES

Abdessalam, H., Abbès, B., Li, Y., Guo, Y.Q., Kwassi, E., Romain, J.L., 2015. Simulation of polyurethane foam expansion with finite pointset and volume of fluid methods: implementation and experimental validation. Mater. Res. Innov. 19, S8-149-S8-156. https://doi.org/10.1179/1432891715Z.0000000001646

Al-Moameri, H., Zhao, Y., Ghoreishi, R., Suppes, G.J., 2015. Simulation of liquid physical blowing agents for forming rigid urethane foams. J. Appl. Polym. Sci. 132, n/a-n/a. https://doi.org/10.1002/app.42454

Baser, S.A., Khakhar, D.V., 1994a. Modeling of the dynamics of R-11 blown polyurethane foam formation. Polym. Eng. Sci. 34, 632–641.

Baser, S.A., Khakhar, D.V., 1994b. Modeling of the Dynamics of Water and R-11 blown polyurethane foam formation. Polym. Eng. Sci. 34, 642–649.

Basso, M.C., Pizzi, A., Celzard, A., 2013a. Dynamic Foaming Behaviour of Polyurethane vs Tannin/Furanic Foams. J. Renew. Mater. 1, 273–278. https://doi.org/10.7569/JRM.2013.634125

Basso, M.C., Pizzi, A., Celzard, A., 2013b. Influence of formulation on the dynamics of preparation of tannin-based foams. Ind. Crops. Prod. 51, 396-400. https://doi.org/10.1016/j.indcrop.2013.09.013

Basso, M.C., Pizzi, A., Celzard, A., 2013c. Dynamic monitoring of tannin-based foam preparation: effects of surfactant. Bioresources 8, 5807-5816.

Basso, M.C., Lagel, M.C., Pizzi, A., Celzard, A. Abdalla, S., 2015. First tools for tannin-furanic foams design. Bioresources 10, 5233-5241.

Bikard, J., Bruchon, J., Coupez, T., Silva, L., 2007. Numerical simulation of 3D polyurethane expansion during manufacturing process. Colloids Surf. Physicochem. Eng. Asp. 309, 49–63. https://doi.org/10.1016/j.colsurfa.2007.04.025

Bikard, J., Bruchon, J., Coupez, T., Vergnes, B., 2005. Numerical prediction of the foam structure of polymeric materials by direct 3D simulation of their expansion by chemical reaction based on a multidomain method. J. Mater. Sci. 40, 5875–5881. https://doi.org/10.1007/s10853-005-5022-9

Bourdon, C.J., Cote, R.O., Moffat, H.K., Grillet, A.M., Mahoney, J.F., Russick, E.M., Adolf, D.B., Rao, R.R., Thompson, K.R., Kraynik, A.M., Castaneda, J.N., Brotherton, C.M., Mondy, L.A., Gorby, A.D., 2008. Experiments for foam model development and validation. (No. SAND2008-6162, 941408). https://doi.org/10.2172/941408

Čop, M., Laborie, M.P., Pizzi, A., Sernek, M., 2014. Curing Characterisation of Spruce Tannin-based Foams using the Advanced Isoconversional Method. BioResources 9. https://doi.org/10.15376/biores.9.3.4643-4655

Dimier, F., Sbirrazzuoli, N., Vergnes, B., Vincent, M., 2002. Etude rhéocinétique d'un système polyuréthane, in: 37ème Congrès Du Groupe Français de Rhéologie. Groupe français de Rhéologie, pp. 6–pages.

Ferkl, P., Karimi, M., Marchisio, D.L., Kosek, J., 2016. Multi-scale modelling of expanding polyurethane foams: Coupling macro- and bubble-scales. Chem. Eng. Sci. 148, 55–64. https://doi.org/10.1016/j.ces.2016.03.040

Geier, S., Winkler, C., Piesche, M., 2009. Numerical Simulation of Mold Filling Processes with Polyurethane Foams. Chem. Eng. Technol. 32, 1438–1447. https://doi.org/10.1002/ceat.200900202

Ghoreishi, R., Zhao, Y., Suppes, G.J., 2014. Reaction modeling of urethane polyols using fraction primary secondary and hindered-secondary hydroxyl content. J. Appl. Polym. Sci. 131. https://doi.org/10.1002/app.40388

Gill, P.E., Murray, W., Saunders, M.A., 2002. SNOPT: An SQP Algorithm for Large-Scale Constrained Optimization. SIAM J. Optim. 12, 979–1006. https://doi.org/10.1137/S1052623499350013

Guigo, N., Mija, A., Vincent, L., Sbirrazzuoli, N., 2007. Chemorheological analysis and model-free kinetics of acid catalysed furfuryl alcohol polymerization. Phys. Chem. Chem. Phys. 9, 5359. https://doi.org/10.1039/b707950h

Gupta, V.K., Khakhar, D.V., 1999. Formation of integral skin polyurethane foams. Polym. Eng. Sci. 39, 164–176. https://doi.org/10.1002/pen.11405

Ireka, I.E., Niedziela, D., Schäfer, K., Tröltzsch, J., Steiner, K., Helbig, F., Chinyoka, T., Kroll, L., 2015. Computational modelling of the complex dynamics of chemically blown polyurethane foam. Phys. Fluids 27, 113102. https://doi.org/10.1063/1.4935788

Karimi, M., Droghetti, H., Marchisio, D.L., 2017. PUFoam: A novel open-source CFD solver for the simulation of polyurethane foams. Comput. Phys. Commun. 217, 138–148.

Karimi, M., Droghetti, H., Marchisio, D.L., 2016. Multiscale Modeling of Expanding Polyurethane Foams via Computational Fluid Dynamics and Population Balance Equation. Macromol. Symp. 360, 108–122. https://doi.org/10.1002/masy.201500108

Lacoste, C., Čop, M., Kemppainen, K., Giovando, S., Pizzi, A., Laborie, M.-P., Sernek, M., Celzard, A., 2015. Biobased foams from condensed tannin extracts from Norway spruce (Picea abies) bark. Ind. Crops Prod. 73, 144–153. https://doi.org/10.1016/j.indcrop.2015.03.089

Lacoste, C., Pizzi, A., Basso, M.-C., Laborie, M.-P., Celzard, A., 2014. Pinus pinaster tannin/furanic foams: PART I. Formulation. Ind. Crops Prod. 52, 450–456. https://doi.org/10.1016/j.indcrop.2013.10.044

Li, Jiongjiong, Zhang, A., Zhang, S., Gao, Q., Zhang, W., Li, Jianzhang, 2019. Larch tannin-based rigid phenolic foam with high compressive strength, low friability, and low thermal conductivity reinforced by cork powder. Compos. Part B Eng. 156, 368–377. https://doi.org/10.1016/j.compositesb.2018.09.005

Marciano, J.H., Reboredo, M.M., Rojas, A.J., Williams, R.J.J., 1986. Integral-skin polyurethane foams. Polym. Eng. Sci. 26, 717–724. https://doi.org/10.1002/pen.760261102

Marciano, J.H., Rojas, A.J., Williams, R.J., 1982. Curing kinetics of a rigid polyurethane foam formulation. Polymer 23, 1489–1492.

Marie, Z., Nicolas, V., Celzard, A., Fierro, V., 2020. First approach for modelling the physical foaming of tannin-based thermoset foams. Int. J. Therm. Sci. 149, 106212. https://doi.org/10.1016/j.ijthermalsci.2019.106212

Marie, Z., Nicolas, V., Celzard, A., Fierro, V., 2019. Experimental investigation of the physical foaming of tannin-based thermoset foams. Ind. Crops Prod. 138, 111424. https://doi.org/10.1016/j.indcrop.2019.05.073

Piloyan, G.O., Ryabchikov, I.D., Novikova, O.S., 1966. Determination of Activation Energies of Chemical Reactions by Differential Thermal Analysis. Nature 212, 1229–1229. https://doi.org/10.1038/2121229a0

Rao, R., Mondy, L., Noble, D., Brunini, V., Long, K., Roberts, C., Wyatt, N., Celina, M., Thompson, K., Tinsley, J., 2018. Density predictions using a finite element/level set model of polyurethane foam expansion and polymerization. Comput. Fluids 175, 20–35. https://doi.org/10.1016/j.compfluid.2018.08.010

Rao, R.R., Mondy, L.A., Long, K.N., Celina, M.C., Wyatt, N., Roberts, C.C., Soehnel, M.M., Brunini, V.E., 2017. The kinetics of polyurethane structural foam formation: Foaming and polymerization. AIChE J. https://doi.org/10.1002/aic.15680

Rao, R.R., Mondy, L.A., Noble, D.R., Moffat, H.K., Adolf, D.B., Notz, P.K., 2012. A level set method to study foam processing: a validation study. Int. J. Numer. Methods Fluids 68, 1362–1392. https://doi.org/10.1002/fld.2671

Seo, D., Youn, J.R., 2005. Numerical analysis on reaction injection molding of polyurethane foam by using a finite volume method. Polymer 46, 6482–6493. https://doi.org/10.1016/j.polymer.2005.03.126

Shen, L., Zhao, Y., Tekeei, A., Hsieh, F.-H., Suppes, G.J., 2014. Density modeling of polyurethane box foam. Polym. Eng. Sci. 54, 1503–1511. https://doi.org/10.1002/pen.23694

Sjöström, E., 1993. Wood chemistry: fundamentals and applications, 2nd ed. ed. Academic Press, San Diego.

Tondi, G., Zhao, W., Pizzi, A., Du, G., Fierro, V., Celzard, A., 2019. Tannin - based rigid foams: a survey of chemical and physical properties. Biores. Technol. 100, 5162-5169. https://doi.org/10.1016/j.biortech.2009.05.055

Zhao, Y., Gordon, M.J., Tekeei, A., Hsieh, F.-H., Suppes, G.J., 2013. Modeling reaction kinetics of rigid polyurethane foaming process. J. Appl. Polym. Sci. 130, 1131–1138. https://doi.org/10.1002/app.39287

Zhao, Y., Suppes, G.J., 2015. Computational study on reaction enthalpies of urethane-forming reactions. Polym. Eng. Sci. 55, 1420–1428. https://doi.org/10.1002/pen.24086

Zhao, Y., Zhong, F., Tekeei, A., Suppes, G.J., 2014. Modeling impact of catalyst loading on polyurethane foam polymerization. Appl. Catal. Gen. 469, 229–238. https://doi.org/10.1016/j.apcata.2013.09.055

Zhou, X., Li, B., Xu, Y., Essawy, H., Wu, Z., Du, G., 2019. Tannin-furanic resin foam reinforced with cellulose nanofibers (CNF). Ind. Crops Prod. 134, 107–112. https://doi.org/10.1016/j.indcrop.2019.03.052